J Solid State Electrochem (2014) 18:1519–1528
DOI 10.1007/s10008-013-2365-z

ORIGINAL PAPER

Glassy carbon electrode modified with a film of poly(Toluidine Blue O) and carbon nanotubes for nitrite detection

Delia Gligor · Alain Walcarius

Received: 26 August 2013 / Revised: 11 December 2013 / Accepted: 12 December 2013 / Published online: 9 January 2014

Abstract This work describes the modification of a glassy carbon electrode with poly(Toluidine Blue O) (GC/poly-TBO) and single-walled carbon nanotubes (SWCNT) for the electrocatalytic oxidation of nitrite. GC/poly-TBO was prepared by electropolymerization and used as such or after immobilizing SWCNT on the polymeric film to give a composite GC/poly-TBO-SWCNT electrode. The electrochemical and catalytic behavior of both electrodes was studied comparatively. It was observed that the presence of SWCNT contributed to enhance the electrocatalytic response for nitrite oxidation, as measured by amperometry at +0.92 V vs. Ag/AgCl/KCl_{sat} and pH 7. The response was linear with respect to the nitrite concentration in the 0.001–4 mM range, with a detection limit of 0.37 μM (based on signal to noise ratio of 3) for GC/poly-TBO-SWCNT. The proposed method was also applied to the determination of nitrite in a wastewater sample and compared to the spectrophotometric method.

Keywords Nitrite · Toluidine Blue · Carbon nanotubes · Amperometric sensor

Introduction

Nitrite (NO_2^-) is an important source of nitrogen in green plants, and its complete reduction is achieved in nature by the nitrite reductase enzyme [1]. It is used as an additive in some types of food, and its occurrence in soils, waters, foods, and physiological systems is prevalent. The presence of excess nitrite in vegetables, drinking water, and food products is a serious threat to human health [2]. Nitrite promotes the irreversible oxidation of hemoglobin and reduces the blood capacity to transport oxygen. Also, it may interact in the stomach with amines and amides forming highly carcinogenic *N*-nitrosamine, many of which are known to be carcinogens. Therefore, NO_2^- determination is of great significance for environment security and public health. Monitoring variations of nitrite is important for understanding their biogeochemical processes in aquatic environments and for developing better methods of managing water quality [3–11].

Many analytical methods have been proposed for nitrite detection, mainly based on spectrophotometry, chromatography, capillary electrophoresis, chemiluminescence, and electrochemistry [12–16]. Most of these methods are often affected by the presence of coexisting cationic or anionic species, and they are either time-consuming or needing sophisticated instruments. Owing to their rapid response, cheap, safe, and simple use, the electrochemical methods have often been employed for nitrite detection. In doing so, chemically modified electrodes have proven to be particularly efficient, in terms of eliminating the effects of interference species and/or by providing suitable electrocatalytic properties likely to improve nitrite oxidation processes, which was notably achieved by modifying the electrode surface with redox mediators [3–11, 17–29]. Various redox mediators (e.g., dyes) were used for to build amperometric sensors for nitrite [30, 31]. On the other hand, the interest of electrodes based on nanocomposites [32, 33] or carbon nanotubes for the detection of bioorganic and inorganic compounds, e.g. nitrites, has been the subject of several previous reports (see, e.g., [34–40]).

In this context, the present paper describes the coverage of glassy carbon (GC) electrodes with a polymeric film of Toluidine Blue O (GC/poly-TBO), as obtained by electropolymerization, and the subsequent modification of GC/poly-TBO with single-walled carbon nanotubes (SWCNT) by immobilization onto the polymeric film to give a composite electrode (GC/poly-TBO-SWCNT). The aim of using carbon nanotubes was to investigate their possible interest to increase the sensitivity for nitrite detection as

D. Gligor (✉)
Department of Environmental Analysis and Engineering, "Babes-Bolyai" University, 400294 Cluj-Napoca, Romania
e-mail: delia.gligor@ubbcluj.ro

A. Walcarius
Laboratoire de Chimie Physique et Microbiologie pour l'Environment, UMR 7564, CNRS—Université de Lorraine, 405 rue de Vandoeuvre, 54600 Villers les Nancy, France

expected from improved electron transport issues. Actually, the catalytic behavior of Toluidine Blue with respect to nitrite oxidation is known [30, 41] and the combined use of Toluidine Blue and carbon nanotubes has been reported for bioelectrocatalytic applications [42–45], but, to date, poly(Toluidine Blue) and carbon nanotubes composite films were not yet described for nitrite detection. The electrochemical and electrocatalytic behavior of both GC/poly-TBO and GC/poly-TBO-SWCNT electrodes toward nitrite oxidation was studied comparatively. This was made by investigating the electrochemical stability and the influence of some experimental parameters on the voltammetric response (pH, scan rate). The obtained electrodes were tested as amperometric sensors for nitrite detection in synthetic and real samples. The nitrite concentration in a real sample (wastewater) was determined using the standard addition method and compared to a standardized procedure (Griess assay).

Experimental

Reagents

Toluidine Blue O (TBO) was purchased from Aldrich (Steinheim, Germany). Single-walled carbon nanotubes (SWCNTs) and sodium tetraborate were obtained from Sigma (St. Louis, MO, USA), while sodium nitrite was purchased from Reactivul Bucharest (Romania). $Na_2HPO_4{\cdot}2H_2O$ and $NaH_2PO_4{\cdot}H_2O$ were purchased from Merck (Darmstadt, Germany).

All reagents were of analytical grade and used as received. The supporting electrolyte was 0.1 M phosphate buffer solution, obtained by mixing solutions of $Na_2HPO_4{\cdot}2H_2O$ and $NaH_2PO_4{\cdot}H_2O$ in appropriate ratios. When necessary, pH was adjusted in the interval of 2–10, using H_3PO_4 or NaOH solutions. The nitrite stock solution used throughout this study was made of 0.1 M $NaNO_2$, which was then diluted to reach the desired concentrations.

The electropolymerization solution (pH 9.1) used to modify the electrodes was composed of $5{\cdot}10^{-4}$ M TBO, 0.1 M $NaNO_3$, and 0.01 M sodium tetraborate [30].

Electrode preparation

Glassy carbon electrodes modified with poly(Toluidine Blue) (GC/poly-TBO)

Prior to electrochemical experiments, GC electrodes (surface area of 0.07 cm^2) were polished with aqueous 0.3 μm alumina slurry on a polishing cloth, followed by subsequent washing for 5 min in an ultrasonic bath with ethanol and water in order to remove any trace impurities. Then the polymer film electrode was prepared by scanning successive cyclic voltammograms of TBO on GC electrode in the potential range between −0.6 and 1.1 V vs. $Ag/AgCl/KCl_{sat}$, at 50 mV s^{-1}, during 20 cycles, in $5{\cdot}10^{-4}$ M TBO solution.

Glassy carbon electrodes modified with poly(Toluidine Blue) and carbon nanotubes (GC/poly-TBO-SWCNT)

The SWCNTs were immobilized onto the GC/poly-TBO electrode by using water as the dispersing agent. The casting solution was prepared by introducing 1 mg of SWCNTs into 200 μL deionized water.

The SWCNT were actually oxidized (giving rise to an oxygen-to-carbon atomic ratio of 6 %, as determined by X-ray photoelectron spectroscopy, exhibiting the typical narrow C1s sp2 main signal at 284.1 eV and a small contribution of C-O moieties at 285.9 eV), bearing enough hydrophilic groups to be quite easy to disperse. Strong sonication was applied and, if aggregates were still present, a rather homogeneous SWCNTs dispersion was achieved. Then 20 μL aliquot of this sonicated suspension was placed directly onto the GC/poly-TBO electrode surface and left to dry, after which the electrode was ready for use. In this way, the GC/poly-TBO-SWCNT electrode was obtained. A microscopic characterization of the proposed modified electrode by SEM revealed deposits with a dendritic-like morphology (Fig. 1a), containing quite regular substructures of submicron size (Fig. 1b–d) into which the SWCNTs are expected to be deposited (not visible by SEM). It is noteworthy that such configuration "electrode/polymer/nanotubes" might be unexpected by comparison to the more conventional "electrode/nanotubes/modifier" configuration, but this latter gave rise to lower sensitivities for the analysis of nitrite (by *ca.* 20 %), so that the sandwich configuration GC/poly-TBO/SWCNT was preferred here.

All presented results are the average one of at least three identically prepared electrodes, if not otherwise mentioned.

Electrochemical measurements

Cyclic voltammetry was performed in a conventional three-electrode system. A platinum wire was used as a counter electrode, $Ag|AgCl/KCl_{sat}$ as a reference electrode, and the modified glassy carbon electrodes (3 mm diameter) as working ones. All electrochemical experiments were carried out using an Autolab electrochemical analyzer (Autolab-PGSTAT 10, Eco Chemie, Utrecht, Netherlands). All measurements were performed at room temperature.

Batch amperometric measurements at various nitrite concentrations were carried out at an applied potential of +960 mV vs. $Ag/AgCl/KCl_{sat}$, under magnetic stirring, using 0.1 M phosphate buffer solution as supporting electrolyte. The current-time data were collected using the above mentioned electrochemical analyzer.

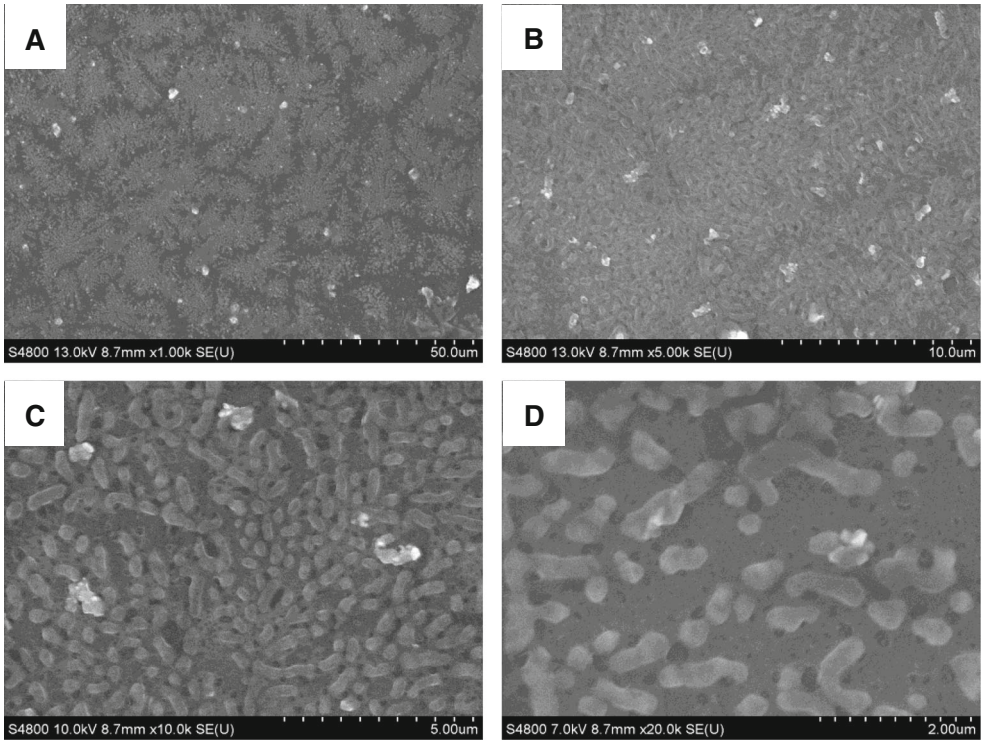

Fig. 1 SEM micrographs of GC/poly-TBO-SWCNT at various magnifications

Spectrophotometric analysis of nitrite was carried out with the UV–Vis spectrophotometer Jasco 615.

Monitoring pH of the phosphate buffer solutions was made using an HI255 pH meter (Hanna Instruments, Romania), with a combined glass electrode.

Results and discussions

Basic electrochemical characterization

Typical cyclic voltammograms recorded for TBO electropolymerization on GC electrode (Fig. 2) are characterized by well-defined voltammetric peaks. From multisweep potential scanning of the GC electrode in the TBO solution, it can be observed that the anodic and cathodic peak currents increased continuously during cycling (Fig. 2), with shape variations in agreement with those previously observed for electrodeposited poly(Toluidine Blue) films [30]. This proves the progressive deposition of a TBO film on the GC surface, as also confirmed by the indigo color specific to TBO on the electrode surface. The application of 20 potential scans for TBO electropolymerization was the optimum condition giving rise to the highest voltammetric signals, in agreement with previous observations made for the electropolymerization of other dyes of related structure (e.g., 25 cycles for brilliant cresyl blue [31]).

Analysis of the obtained poly-TBO-modified electrodes without (GC/poly-TBO) or with carbon nanotubes (GC/poly-TBO-SWCNT) by cyclic voltammetry in phosphate buffer (pH 7, 10 mV s^{-1}, see plain curves in parts A and B of Fig. 3) reveals the existence of peak pairs characterized by quasi-reversible $2e^-$ transfer processes (ΔE_p=0.14 V for GC/poly-TBO and 0.08 V for GC/poly-TBO-SWCNT). Values of formal standard potentials, $E^{0'}$, of such adsorbed mediator (evaluated as average of anodic and cathodic peak potentials) are −0.01 V vs. $Ag/AgCl/KCl_{sat}$ for GC/poly-TBO and −0.04 V vs. $Ag/AgCl/KCl_{sat}$ for GC/poly-TBO-SWCNT. The amount of electroactive TBO moieties was slightly larger in the presence of carbon nanotubes, resulting in higher apparent

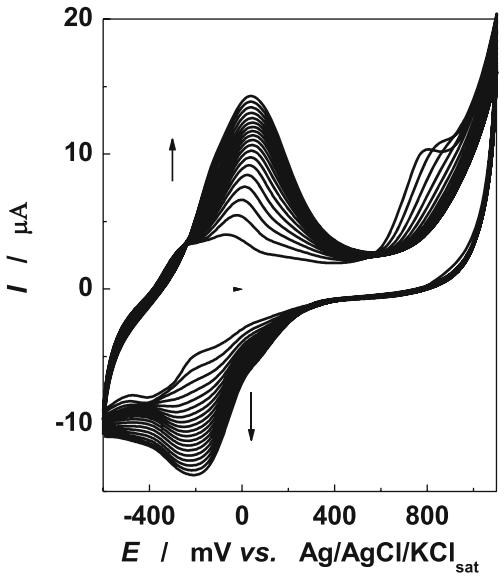

Fig. 2 Cyclic voltammograms recorded at 50 mV s^{-1} for TBO electropolymerization on GC electrode (solution: $5{\cdot}10^{-4}$ M TBO, 0.1 M $NaNO_3$, and 0.01 M sodium tetraborate)

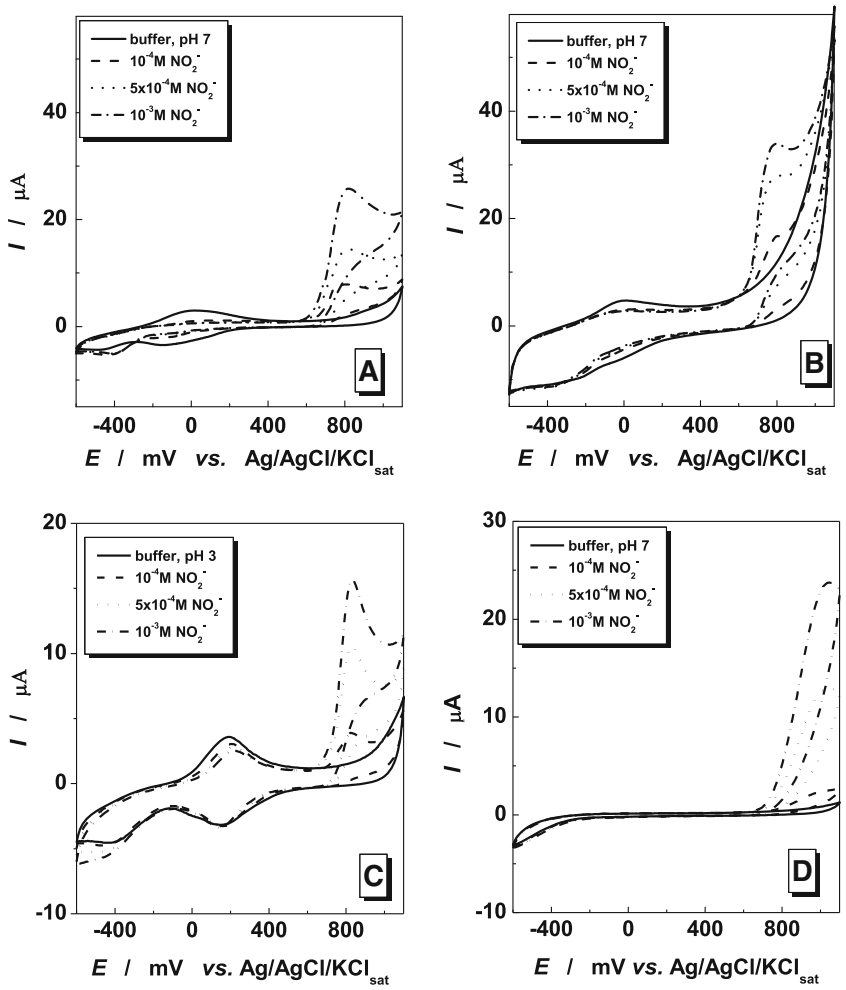

Fig. 3 Cyclic voltammograms obtained at 10 mV s^{-1} using GC/poly-TBO (**a** at pH 7), GC/poly-TBO-SWCNT (**b** at pH 7; **c** at pH 3) and unmodified GCE (**d**), respectively, without (*plain curves*) and with increasing concentrations of nitrite in the medium

surface coverage (Γ_{app}=6.8×10^{-10} mol cm^{-2} for GC/poly-TBO and 15.3×10^{-10} mol cm^{-2} for GC/poly-TBO-SWCNT).

Actually, the values of surface coverage are related to the electropolymerization conditions. We even obtained, in other cases, smaller surface coverages (of 10^{-12} order), as in [46]. Here, the coverage corresponds to ca. 5–10 TBO units per square nanometer, so that we do have a very thin coating layer of few monolayers.

It can be concluded from these results that using SWCNT has a beneficial effect on the electrochemical behavior of the modified electrodes (lower ΔE_p value and a higher amount of electroactive TBO). Also, it can be observed that the GC/poly-TBO-SWCNT-modified electrodes exhibit a negative shift of the $E^{0'}$ value, which can be attributed to a specific feature of CNT-modified electrodes [34].

As expected for surface-confined redox species, the cyclic voltammograms recorded at various potential scan rates (in the range of 0.01–6.4 V s^{-1}) presented a linear dependence of peak current intensity (I_p) on scan rate (v) (results not shown). The slopes of log I_p vs. log v dependencies were close to the theoretical value of one, confirming the existence of adsorbed species. From such measurements performed at different scan rates, the heterogeneous electron transfer rate constants, k_s, and transfer coefficients, α, were calculated using the method proposed by Laviron [47], from the variation of the peak potentials with the potential scan rate and based on the Eqs. (1) and (2). The values for k_s increases in the sequence: 17.4 s^{-1} (pH 3)< 73.9 s^{-1} (pH 7)<94.9 s^{-1} (pH 9) for GC/poly-TBO. For GC/poly-TBO-SWCNT, the k_s value was 97.4 s^{-1} at pH 7.

It can be observed that the value of k_s constant for GC/poly-TBO-SWCNT electrode is slightly higher than for GC/poly-TBO in phosphate buffer at pH 7.

$$E_{pc}-E^{0'}=\frac{RT}{\alpha nF}\cdot 2.3\log\frac{\alpha nF}{RTk_s}+\frac{2.3RT}{\alpha nF}\log v \quad (1)$$

$$E_{pa}-E^{0'}=\frac{RT}{(1-\alpha)nF}\cdot 2.3\log\frac{(1-\alpha)nF}{RTk_s}+\frac{2.3RT}{(1-\alpha)nF}\log v \quad (2)$$

The values of k_s appear rather high in contrast to the CV curves presented in Fig. 3, but these values depend also on the surface coverage. Note that values for k_s as high as 135 s^{-1} have been reported for a system that was not reversible (see [48]).

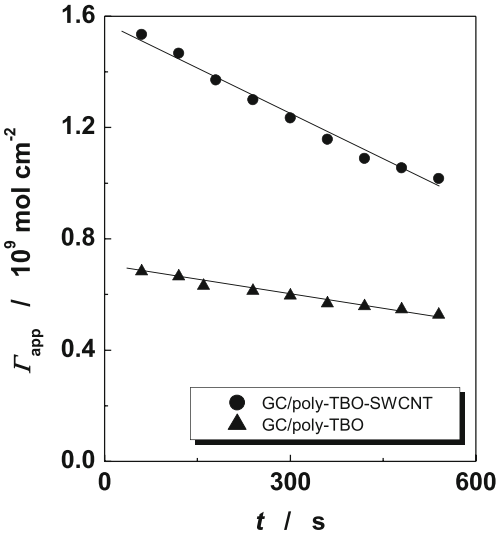

Fig. 4 Linear dependence of surface coverage Γ vs. cycling time for GC/poly-TBO and GC/poly-TBO-SWCNT. Experimental conditions: starting potential, −600 mV vs. Ag/AgCl/KCl_{sat}; scan rate, 50 mV s^{-1}; supporting electrolyte, 0.1 M phosphate buffer, pH 7

Also, the aforementioned k_s values suggest an influence of pH, which was especially studied for the GC/poly-TBO electrode (GC/poly-TBO-SWCNT being only used for comparison purpose at the optimum pH 7). Actually, not only electron transfer rate parameters were affected by pH but also the voltammetric peak potentials were pH dependent (compare the plain curves in parts B and C of Fig. 3). Within the pH range investigated here (from 3 to 9), the $E^{0'}$ vs. pH dependence was linear, with a slope of 0.038 V/ΔpH ($E^{0'}$=0.26+ 0.038 pH; R (correlation coefficient)/N (no. of experimental points)=0.961/7). This suggests the existence of a redox process involving $2e^-/2H^+$ in accordance with literature data [30].

pH was also found to affect the apparent surface coverage (i.e., the amount of electroactive TBO species per surface unit) and the stability of the electrode response upon continuous potential scanning. Stability tests of investigated systems were realized in potentiodynamic conditions: the potential of modified electrodes was scanning in the potential range covering the redox activity of mediator, with the scan rate of 50 mV s^{-1}, during 20 cycles, in phosphate buffer solution of pH 3, pH 5, pH 7, and pH 9 for GC/poly-TBO and in phosphate buffer solution of pH 7 for GC/poly-TBO-SWCNT. Actually, pH 7 was the best compromise between good sensitivity and acceptable stability. As observed for GC/poly-TBO, at pH 5 and pH 9, the peaks almost vanished after 20 cycles, whereas data obtained at pH 3 revealed a quite good stability but very low sensitivity (Γ_{app} values 4–5 times lower than for the pH range of 5–9). Further experiments will be thus performed at pH 7. It should be also noted that if Γ_{app} was 2–3 times higher for GC/poly-TBO-SWCNT than for GC/poly-TBO (as mentioned above), it tended to deactivate more rapidly. The deactivation rate constants, k_{deact}, as calculated from the slope of Eq. 3 (variation of Γ_{app} values with time of potential scanning, see Fig. 4), were 3.3×10^{-12} mol cm^{-2} s^{-1} and 1.1×10^{-11} mol cm^{-2} s^{-1}, respectively, for GC/poly-TBO and GC/poly-TBO-SWCNT.

$$\Gamma_{app} = \Gamma_{app\ (t=0)} - k_{deact} t \quad (3)$$

Based on the good electrochemical stability observed for GC/poly-TBO-SWCNT (expressed by a low value of deactivation rate constant: 1.1×10^{-11} mol cm^{-2} s^{-1}), one can assume a rather durable immobilization of SWCNTs on the electrode surface.

Electrochemical response to nitrite

Cyclic voltammetry evidence of catalytic properties

Figure 3 presents the cyclic voltammograms corresponding to GC/poly-TBO (part A) and GC/poly-TBO-SWCNT (part B at pH 7 and part C at pH 3). As can be observed, in the presence

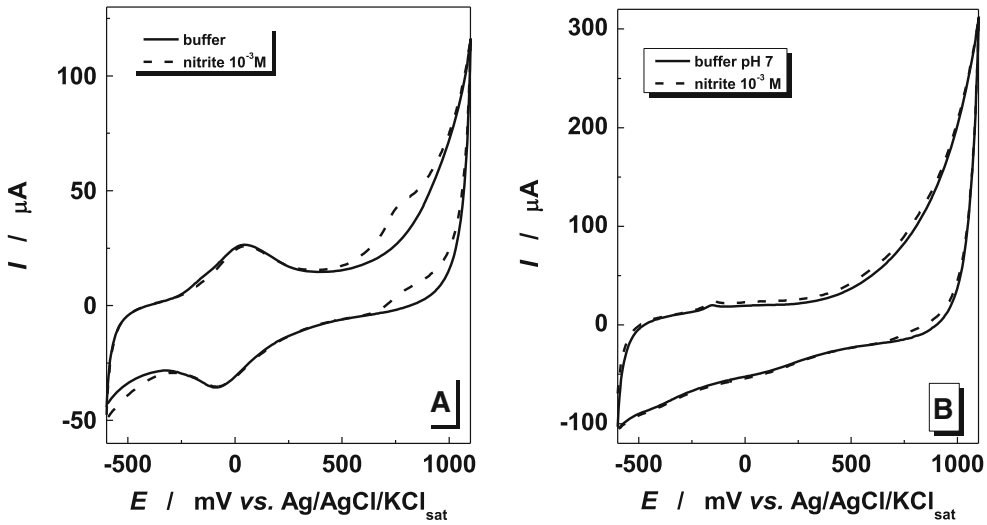

Fig. 5 Cyclic voltammograms obtained at 10 mV s^{-1} using GC/SWCNT/poly-TBO (**a**) and GC/SWCNT (**b**), respectively, without (*plain curves*) and with 10^{-3} M nitrite in the medium (*dashed curves*)

Table 1 Analytical parameters corresponding to amperometric calibration curves for nitrite detection, using GC/poly-TBO and GC/poly-TBO-SWCNT electrodes (pH was adjusted using 0.1 M phosphate buffer solutions)

Electrode	pH	Linear calibration				log *I*–log *c* dependence	
		DL (μM)	*S* (mA M^{-1} cm^{-2})	Linear range (mM)	*R*/*N*	Slope	*R*/*N*
GC/poly-TBO	3	0.55	31.4	0.001–2	0.997/14	0.90±0.02	0.095/18
GC/poly-TBO	7	0.90	50	0.01–0.8	0.996/15	0.98±0.03	0.991/20
GC/poly-TBO-SWCNT	3	0.10	70	0.001–0.4	0.999/20	1.03±0.01	0.998/21
GC/poly-TBO-SWCNT	7	0.37	84.3	0.001–4	0.999/23	0.99±0.01	0.994/23

DL detection limit, *S* sensitivity, *N* no. of experimental points

of nitrite, an oxidation peak starts to grow at ca. +0.60 V to reach a maximum at +0.80 V, which significantly increases with nitrite concentration. By comparison to the unmodified GC electrode (Fig. 3d), these signals are slightly shifted toward lower overpotentials (i.e., the oxidation peak starts to grow at ca. +0.70 V on unmodified GC and reach a maximum at +0.90 V), suggesting a favorable electrocatalytic effect due to the presence of TBO onto the electrode surface. The rather small shift in the observed overpotentials with respect to the unmodified electrode is consistent with previous observations for similar mediators applied to nitrite detection [30, 31]. Actually, the oxidation of nitrite is quite complex at glassy carbon electrode and usually better defined in acidic medium [49], but all further investigations were preferably made in neutral pH here because this pH is more appropriate for amperometric nitrite detection in real samples. In addition, comparing the responses of GC/poly-TBO and GC/poly-TBO-SWCNT also features a slightly better electrocatalytic behavior for GC/poly-TBO-SWCNT (lower overpotentials by ca. 30 mV) as well as some increase in sensitivity for nitrite detection in the presence of SWCNTs (compare parts A and B in Fig. 3), yet with larger capacitive currents as expected from the increased electroactive surface area when CNTs are present onto the electrode surface. This latter effect should be overcome when working in amperometric conditions, as discussed in section "Amperometric detection of nitrite ions." Note that this GC/poly-TBO-SWCNT configuration gave rise to larger electrocatalytic peak enhancement than the GC/SWCNT-poly-TBO one (compare Figs. 3b and 5a).

From the mechanistic point of view, it appears clearly that the electrocatalytic effect is due to the poly-TBO (i.e., no significant electrocatalytic effect of SWCNT, see control experiment in Fig. 5b) and that the presence of SWCNT only adds an additional effect of sensitivity enhancement, which might be explained by their high specific surface area and good conductivity (contributing thereby to improve the electrocatalytic behavior of poly-TBO). The possible electrocatalytic process is thus expected to operate as previously described [30] and can be expressed as follows:

$$\text{poly} - \text{TBOH}^+ + \text{NO}_2^- \rightarrow \text{poly} - \text{TBOH}^+ \cdot \text{NO}_2^-$$
$$\text{poly} - \text{TBOH}^+ \cdot \text{NO}_2^- + \text{H}_2\text{O} \rightarrow \text{poly}-\text{TBOH}^+ \cdot \text{NO}_3^- + 2\text{H}^+ + 2\text{e}^-$$
$$\text{poly} - \text{TBOH}^+ \cdot \text{NO}_3^- \rightarrow \text{poly} - \text{TBOH}^+ + \text{NO}_3^-$$

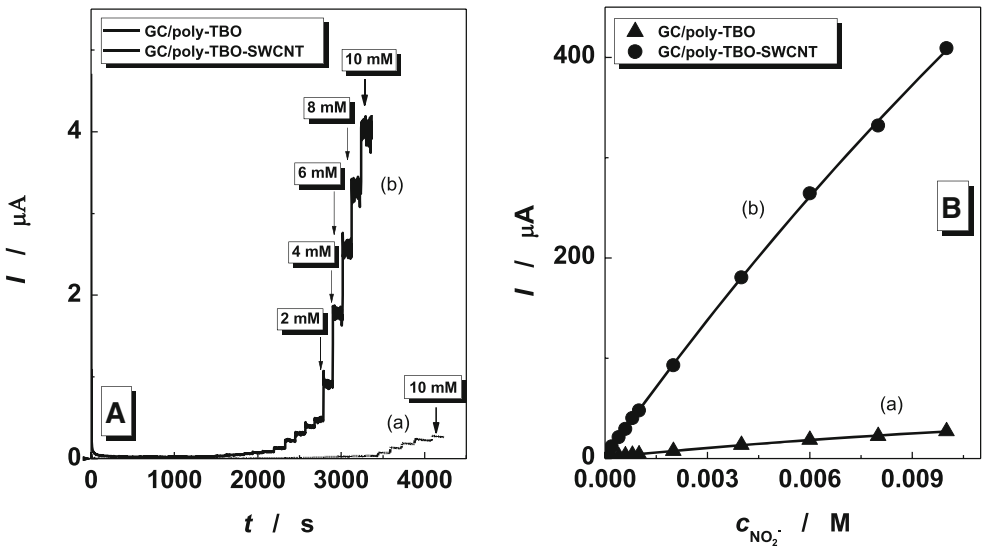

Fig. 6 *I*–*t* (**a**) and corresponding calibration (**b**) curves for nitrite, as measured using GC/poly-TBO (*a*) and GC/poly-TBO-SWCNT (*b*). Experimental conditions: applied potential, +920 mV vs. $Ag/AgCl/KCl_{sat}$; supporting electrolyte, 0.1 M phosphate buffer solution, pH 7. Every step in *I*–*t* curves corresponds to a final concentration of nitrite, and this is obtained by using the same calculation as in Fig. 4a, curve *b*, the last five steps (the previous steps for curve *b* are 1, 0.8, 0.6, 0.4, 0.2, 0.1, 0.08, 0.06, 0.04, and 0.02 mM, etc.)

Amperometric detection of nitrite ions

The amperometric measurements were performed in stationary regime, at an applied potential of +0.92 V vs. Ag/AgCl/KCl_{sat}, at two pH values (3 and 7) in magnetically stirred solutions. The main analytical parameters are presented in Table 1. The detection limit was calculated as signal/noise ratio of 3, from a current vs. time curve corresponding to the analysis of nitrite at a concentration of 8×10^{-5} M (Fig. 6). Figure 6a illustrates typical amperometric signals recorded for the analysis of nitrite at increasing concentrations at pH 7 (as well as the corresponding calibration curves in Fig. 6b). The results clearly show much better sensitivity for GC/poly-TBO-SWCNT in comparison to GC/poly-TBO (compare curves "a" and "b" in Fig. 4), confirming again the improving role of carbon nanotubes in close contact to the polymer. Also, from successive calibration experiments in the presence of SWCNTs, it was observed that the analytical parameters remained almost at the same values (if ten repetitive measurements were made in 1 day, the sensor losts ~2 % of the initial response). This confirmed once again that SWCNT adhered to the polymer, most probably via favorable hydrophobic interactions.

It can be observed from data in Table 1 that the pH solution significantly influences the linear regression parameters for GC/poly-TBO and GC/poly-TBO-SWCNT. The best detection limit (0.1 μM) was obtained with GC/poly-TBO-SWCNT-modified electrode at pH 3, but the obtained results prove that both types of modified electrodes constitute quite good detectors for nitrite, owing to their relatively low

Table 2 A comparison of analytical detection parameters obtained with various modified electrodes in the literature for electrocatalytic detection of nitrite

Electrode	Detection limit (M)	Sensitivity (mA M^{-1})	Linear range (M)	Ref.
GC/Hb/AuNPs/PTH/PtNPs	2×10^{-8}	–	7×10^{-8}–1.2×10^{-3}	[4]
EPPG/SWCNT-PB	6.3×10^{-6}	251.6	3.2×10^{-5}–2.5×10^{-4}	[7]
CPE/L-SCMNPs	6.2×10^{-7}	4840	9.1×10^{-7}–1.3×10^{-4}	[8]
GC/AgNP	1.2×10^{-6}	–	10^{-5}–10^{-3}	[9]
GC/CNF/hemin	3.18×10^{-4}	0.84	5.0×10^{-3}–2.5×10^{-1}	[10]
CS-PB/GNS–CNS	10^{-9}	30.7	2.0×10^{-9}–3.9×10^{-4}	[11]
Pt/CA	5×10^{-7}	0.1	1.0×10^{-6}–1.0×10^{-4}	[19]
Pt/poly(1,8-DAN)	1×10^{-7}	0.7	5.0×10^{-7}–1.0×10^{-4}	
GC/p-NiTAPc	1×10^{-7}	–	5.0×10^{-7}–8.0×10^{-3}	[20]
GC/FeT4MPyP/CoTSPc	4×10^{-8}	370	2.0×10^{-7}–8.6×10^{-6}	[22]
GC/nano-Au/P3MT	2.3×10^{-6}	–	1.0×10^{-5}–1.0×10^{-3}	[24]
GC/CuTSPc/PLL	3.6×10^{-8}	830	1.2×10^{-7}–1.2×10^{-5}	[25]
GC/TBO	5.0×10^{-8}	470	1.0×10^{-7}–1.5×10^{-5}	[30]
GC/BCB	1.0×10^{-7}	12.1	9.0×10^{-7}–1.5×10^{-5}	[31]
GC/nano-Al_2O_3	1.0×10^{-8}	–	5.0×10^{-8}–1.1×10^{-3}	[32]
CPEs/Au-Py/AlSi	1.3×10^{-6}	71.9	7.9×10^{-5}–7.4×10^{-4}	[33]
CPEs/Au-Db/AlSi	3.0×10^{-6}	53.7		
GC/OMIMPF6-MWNT gel Chi	1.0×10^{-8}	739	2.0×10^{-8}–6.0×10^{-5}	[39]
GC/Cyt C/DNA/MWNT-PAMAM Chit	3.0×10^{-8}	–	2.0×10^{-7}–8.0×10^{-5}	[40]
GC/poly-TBO-SWCNT	3.7×10^{-7}	84.3	1.0×10^{-6}–4.0×10^{-3}	This work

GC/AuNPs/PTH/PtNPs hemoglobin immobilized on gold nanoparticles/polythionine/platinum nanoparticles modified glassy carbon electrode, *EPPG/SWCNT-PB* single-walled carbon nanotubes-Prussian blue hybrid-modified edge plane pyrolytic graphite, *CPE/L-SCMNPs* nanocomposite 3,6-bis(2-[2-sulfanyl-ethylimino-methyl]-4-(4-nitro-phenylazo)-phenol)pyridazine-coated SiO2@Fe3O4-modified carbon paste electrode, *GC/AgNP* silver nanoplate-modified glassy carbon electrode, *GC/CNF/hemin* carbon nanofiber hemin-modified glassy carbon electrode, *CS-PB/GNS–CNS* chitosan-coated Prussian blue nanoparticles with the mixture of graphene nanosheets and carbon nanospheres, *Pt/CA* platinum electrodes modified with a cellulose acetate membrane, *Pt/poly(1,8-DAN)* platinum electrodes modified with a poly(1,8-diaminonaphthalene) film, *GC/p-NiTAPc* nikel tetraaminothphalocyanine film-coated glassy carbon electrode, *GC/FeT4MPyP/CoTSPc* glassy carbon electrode modified with alternated layers of iron(III) tetra-(*N*-methyl-4-pyridyl)-porphyrin and cobalt(II) tetrasulfonated phthalocyanine, *GC/nano-Au/P3MT* gold nanoparticles on poly(3GC/Cyt -methylthiophene)-modified glassy carbon electrode, *GC/CuTSPc/PLL* glassy carbon electrode modified with copper tetrasulfonated phthalocyanine immobilized by polycationic poly-L-lysine film, *GC/TBO* glassy carbon electrode modified with Toluidine Blue O, *GC/BCB* glassy carbon electrode modified with brilliant cresyl blue, *GC/nano-Al_2O_3* nano-alumina-modified glassy carbon electrode, *CPEs/Au-Py/AlSi* and *CPEs/Au-Db/AlSi* carbon paste electrodes modified with gold nanoparticles prepared in an aqueous medium using two charged silsesquioxanes, the propylpyridinium chloride and propyl-1-azonia-4-azabicyclo[2.2.2]octane chloride, *GC/OMIMPF6-MWNT gel Chi* ionic liquid (i.e., 1-octyl-3-methylimidazolium hexafluorophosphate, OMIMPF6)-multiwall carbon nanotube (MWNT) gel–chitosan (Chi) composite-modified glassy carbon electrode, *GC/Cyt C/DNA/MWNT-PAMAM Chit* multi-walled carbon nanotubes–poly(amidoamine)–chitosan incorporated DNA and cytochrome c-modified glassy carbon electrode

detection limits. Good response time was also observed as the amperometric response reached 95 % of the steady-state value within ca. 4 s after the addition of nitrite. Compared with previous works [30], the present system enables to work at less anodic values (operating potential lower by ca. 200 mV here) but still suffers from lower sensitivity.

Table 2 compares the analytical performance of amperometric sensors for nitrite, such as sensitivity, linear range, and detection limit, based on other modified electrodes reported in the literature. As it can be seen from Table 2, all the analytical performance obtained for the GC/poly-TBO-SWCNT sensor presented here is comparable with that obtained in previous reports and sometimes even better.

On the other hand, as expected for such modified electrodes, in the whole studied concentration range for reaction of nitrite electrocatalytic oxidation, the apparent reaction order toward nitrite was very close to unity (see the slope of log *I* vs. log *C* dependence from Table 1, as determined in the concentration range corresponding to linear domain of amperometric response). This proves that in all cases the nitrite sensors work under kinetic control, corresponding to reaction order 1 between nitrite and the immobilized mediator. It can be observed that the GC/poly-TBO-SWCNT offered the best performance, confirming again the beneficial effects of CNTs in enhancing reaction rates for nitrite oxidation.

The stability of the modified electrodes was finally investigated. Both modified electrodes present excellent long-term stability under continuous use. They lost ~5 % of their initial response after storage for 4 weeks in 0.1 mM nitrite and ~2 % after storage of a week in 0.1 mM nitrite.

Several chemical species were investigated with respect to their possible interference in the amperometric determination of nitrite. The results showed that 100-fold SO_4^{2-}, CO_3^{2-}, Cl^-, NO_3^-, Ca^{2+}, and Mg^{2+} had no noticeable effect (<1 % for most species, ~3 % for CO_3^{2-}) on the current responses of 0.1 mM nitrite. These results showed that the obtained amperometric sensors possessed high selectivity.

Determination of nitrite in a wastewater sample

The GC/poly-TBO-SWCNT sensor was tested for the detection of nitrite in a wastewater sample obtained from a company of milk products, using the standard addition method. The real sample was diluted by 100 to fall within the linear range of the calibration curve, the applied potential was +0.92 V vs. $Ag/AgCl/KCl_{sat}$ and pH was adjusted to 7. The obtained nitrite concentration in that sample was 60.6 mM. This value is very close to that obtained when analyzing the same wastewater sample using the Griess protocol [50] (i.e., 61.3 mM). The good agreement between the results obtained using the spectrophotometric method and those from the electrochemical method shows the possibility to use this sensor for nitrite determination in real samples.

Conclusions

This work has demonstrated that the immobilization of single-walled carbon nanotubes onto glassy carbon electrodes modified with a polymeric film of Toluidine Blue O contributes to improve the catalytic behavior of the mediator layer toward nitrite oxidation. Both pH effects (potential shifts, variations in sensitivity, and heterogeneous rate constants) and good stability have been evidenced. The obtained modified electrodes can be used as amperometric sensors for nitrite detection. Kinetic parameters were determined from the calibration curves, and the best sensitivity was obtained for GC-poly-TBO-SWCNT (5.85 mA M^{-1}). The obtained sensors have been successfully applied to the determination of nitrite concentration in a wastewater sample, using the standard addition method, and the results were confirmed by comparison to the classical spectrophotometric method.

Acknowledgments We would like to thank to Violeta Gruia (Technische Universitaet Ilmenau, Germany) for performing SEM images and Aurélien Renard for XPS analysis.

References

1. Brittain T, Blackmore R, Greenwood C, Thomson AJ (1992) Bacterial nitrite-reducing enzymes. Eur J Biochem 209:793–802
2. Valcarcel M, Luque de Castro MD (1999) Non-chromatographic continuous separation technique. The Royal Society of Chemistry, Cambridge
3. Amine A, Palleschi G (2004) Phosphate, nitrate, and sulfate biosensors. Anal Lett 37:1–19
4. Zhang Y, Yuan R, Chai Y, Wang J, Zhong H (2011) Amperometric biosensor for nitrite and hydrogen peroxide based on hemoglobin immobilized on gold nanoparticles/polythionine/platinum nanoparticles modified glassy carbon electrode. J Chem Technol Biotechnol 87:570–574
5. Nezamzadeh-Ejhieh A, Nematollahi Z (2011) Surfactant modified zeolite carbon paste electrode (SMZ-CPE) as a nitrate selective electrode. Electrochim Acta 56:8334–8341
6. Meng Z, Liu B, Zheng J, Sheng Q, Zhang H (2011) Electrodeposition of cobalt oxide nanoparticles on carbon nanotubes, and their electrocatalytic properties for nitrite electrooxidation. Microchim Acta 175: 251–257
7. Adekunle AS, Mamba BB, Agboola BO, Ozoemena KI (2011) Nitrite electrochemical sensor based on prussian blue/single-walled carbon nanotubes modified pyrolytic graphite electrode. Int J Electrochem Sci 6:4388–4403
8. Afkhami A, Madrakian T, Ghaedi H, Khanmohammadi H (2012) Construction of a chemically modified electrode for the selective determination of nitrite and nitrate ions based on a new nanocomposite. Electrochim Acta 66:255–264
9. Wang Z, Liao F, Guo T, Yang S, Zeng C (2012) Synthesis of crystalline silver nanoplates and their application for detection of nitrite in foods. J Electroanal Chem 664:135–138
10. Valentini F, Cristofanelli L, Carbone M, Palleschi G (2012) Glassy carbon electrodes modified with hemin-carbon nanomaterial films for amperometric H_2O_2 and NO_2^- detection. Electrochim Acta 63:37–46
11. Cui L, Zhu J, Meng X, Yin H, Pan X, Ai S (2012) Controlled chitosan coated prussian blue nanoparticles with the mixture of graphene

nanosheets and carbon nanoshperes as a redox mediator for the electrochemical oxidation of nitrite. Sensors Actuators B 161:641–647
12. Frenzel W, Schulz-Brussel J, Zinvirt B (2004) Characterisation of a gas-diffusion membrane-based optical flow-through sensor exemplified by the determination of nitrite. Talanta 64:278–282
13. Connolly D, Paull B (2001) Rapid determination of nitrate and nitrite in drinking water samples using ion-interaction liquid chromatography. Anal Chim Acta 441:53–62
14. Mikuska P, Vecera Z (2003) Simultaneous determination of nitrite and nitrate in water by chemiluminescent flow-injection analysis. Anal Chim Acta 495:225–232
15. Lu GH, Jin H, Song DD (1997) Determination of trace nitrite by anodic stripping voltammetry. Food Chem 59:583–587
16. Miyado T, Tanaka Y, Nagai H, Takeda S, Saito K, Fukushi K, Yoshida Y (2004) Simultaneous determination of nitrate and nitrite in biological fluids by capillary electrophoresis and preliminary study on their determination by microchip capillary electrophoresis. J Chromatogr A 1051:185–191
17. Stanley MA, Maxwell J, Forrestal M, Doherty AP, MacCraith BD, Diamond D, Vos JG (1994) Comparison of the analytical capabilities of an amperometric and an optical sensor for the determination of nitrates in river and well water. Anal Chim Acta 299:81–90
18. Pei J, Li XY (2000) Electrochemical study and flow-injection amperometric detection of trace NO(2)(−) at CuPtCl(6) chemically modified electrode. Talanta 51:1107–1115
19. Badea M, Amine A, Palleschi G, Moscone D, Volpe G, Curulli A (2001) New electrochemical sensors for detection of nitrites and nitrates. J Electroanal Chem 59:66–72
20. Wen ZH, Kang TF (2004) Determination of nitrite using sensors based on nickel phthalocyanine polymer modified electrodes. Talanta 62:351–355
21. Xie F, Li W, He J, Yu S, Fu T, Yang H (2004) Directly immobilize polycation bearing Os complexes on mesoporous material MAS-5 and its electrocatalytic activity for nitrite. Mater Chem Phys 86:425–429
22. Santos WJR, Sousa AL, Luz RCS, Damos FS, Kubota LT, Tanaka AA, Tanaka SMCN (2006) Amperometric sensor for nitrite using a glassy carbon electrode modified with alternating layers of iron(III) tetra-(*N*-methyl-4-pyridyl)-porphyrin and cobalt(II) tetrasulfonated phthalocyanine. Talanta 70:588–594
23. Biagiotti V, Valentini F, Tamburri E, Terranova ML, Moscone D, Palleschi G (2007) Synthesis and characterization of polymeric films and nanotubule nets used to assemble selective sensors for nitrite detection in drinking water. Sensors Actuators B 122:236–242
24. Huang X, Li Y, Chen Y, Wang L (2008) Electrochemical determination of nitrite and iodate by use of gold nanoparticles/poly(3-methylthiophene) composites coated glassy carbon electrode. Sensors Actuators B 134:780–786
25. Sousa AL, Santos WJR, Luz RCS, Damos FS, Kubota LT, Tanaka AA, Tanaka SMCN (2008) Amperometric sensor for nitrite based on copper tetrasulphonated phthalocyanine immobilized with poly-L-lysine film. Talanta 75:333–338
26. Salimi A, Hallaj R, Mamkhezri H, Hosaini SMT (2008) Electrochemical properties and electrocatalytic activity of FAD immobilized onto cobalt oxide nanoparticles: application to nitrite detection. J Electroanal Chem 619:31–38
27. Zhu N, Xu Q, Li S, Gao H (2009) Electrochemical determination of nitrite based on poly(amidoamine) dendrimer-modified carbon nanotubes for nitrite oxidation. Electrochem Commun 11:2308–2311
28. Lin CY, Balamurugan A, Lai YH, Ho KC (2010) A novel poly(3,4-ethylenedioxythiophene)/iron phthalocyanine/multi-wall carbon nanotubes nanocomposite with high electrocatalytic activity for nitrite oxidation. Talanta 82:1905–1911
29. Dreyse P, Isaacs M, Calfumán K, Cáceres C, Aliaga A, Aguirre MJ, Villagra D (2011) Electrochemical reduction of nitrite at poly-[Ru(5-NO2-phen)2Cl] tetrapyridylporphyrin glassy carbon modified electrode. Electrochim Acta 56:5230–5237
30. Yang C, Xu J, Hu S (2007) Development of a novel nitrite amperometric sensor based on poly(toluidine blue) film electrode. J Solid State Electrochem 11:514–518
31. Yang C, Lu Q, Hu S (2006) A novel nitrite amperometric sensor and its application in food analysis. Electroanalysis 22:2188–2193
32. He Q, Gan T, Zheng DY, Hu SS (2010) Direct electrochemistry and electrocatalysis of nitrite based on nano-alumina-modified electrode. J Solid State Electrochem 14:1057–1064
33. De Menezes EW, Nunes MR, Arenas LT, Dias SLP, Garcia ITS, Gushikem Y, Costa TMH, Benvenutti EV (2012) Gold nanoparticle/charged silsesquioxane films immobilized onto Al/SiO_2 surface applied on the electrooxidation of nitrite. J Solid State Electrochem 16:3703–3713
34. Wang J, Li M, Shi Z, Li N, Gu Z (2001) Electrocatalytic oxidation of 3,4-dihydroxyphenylacetic acid at a glassy carbon electrode modified with single-wall carbon nanotubes. Electrochim Acta 47:651–657
35. Wang J, Li M, Shi Z, Li N, Gu Z (2002) Direct electrochemistry of cytochrome C at a glassy carbon electrode modified with single-wall carbon nanotubes. Anal Chem 74:1993–1997
36. Yun Y, Dong Z, Shanov V, Heineman WR, Halsall HB, Bhattachary A, Conforti L, Narayan RK, Ball WS, Schulza MJ (2007) Carbon nanotube electrodes and biosensors. NanoToday 2:30–37
37. Qui JD, Zhou WM, Guo J, Wang R, Liang RP (2009) Amperometric sensor based on ferrocene-modified multiwalled carbon nanotube nanocomposites as electron mediator for the determination of glucose. Anal Biochem 385:264–269
38. Gligor D, Varodi C, Muresan LM (2010) Graphite electrode modified with a new phenothiazine derivative and with carbon nanotubes for NADH electrocatalytic oxidation. Chem Biochem Eng Q 24:159–166
39. Xiao F, Liu L, Li J, Zeng J, Zeng B (2008) Electrocatalytic oxidation and voltammetric determination of nitrite on hydrophobic ionic liquid-carbon nanotube gel-chitosan composite modified electrodes. Electroanalysis 20:2047–2054
40. Chen Q, Ai S, Fan H, Cai J, Ma Q, Zhu X, Yin H (2010) The immobilization of cytochrome c on MWNT–PAMAM–Chit nanocomposite incorporated with DNA biocomposite film modified glassy carbon electrode for the determination of nitrite. J Solid State Electrochem 14:1681–1688
41. Thenmozhi K, Narayanan SS (2007) Electrocatalytic reduction of nitrite ion on a toluidine blue sol–gel thin film electrode derived from 3-aminopropyl trimethoxy silane. Electroanalysis 19:2362–2368
42. Lawrence NS, Wang J (2006) Chemical adsorption of phenothiazine dyes onto carbon nanotubes: toward the low potential detection of NADH. Electrochem Commun 8:71–76
43. Yao YL, Shiu KK (2007) Low potential detection of glucose at carbon nanotube modified glassy carbon electrode with electropolymerized poly(toluidine blue O) film. Electrochim Acta 53:278–284
44. Liu Y, Lei J, Ju H (2008) Amperometric sensor for hydrogen peroxide based on electric wire composed of horseradish peroxidase and toluidine blue-multiwalled carbon nanotubes nanocomposite. Talanta 74:965–970
45. Jeykumari DRS, Narayanan SS (2009) Functionalized carbon nanotube-bienzyme biocomposite for amperometric sensing. Carbon 47:957–996
46. Gligor D, Dilgin Y, Popescu IC, Gorton L (2009) Poly-phenothiazine derivative-modified glassy carbon electrode for NADH electrocatalytic oxidation. Electrochim Acta 54:3124–3128
47. Laviron E, Roulier L (1980) General expression of the linear potential sweep voltammogram for a surface redox reaction with interactions

between the adsorbed molecules: applications to modified electrodes. J Electroanal Chem 115:65–74
48. Dicu D, Muresan L, Popescu IC, Cristea C, Silberg IA, Brouant P (2000) Modified electrodes with new phenothiazine derivatives for electrocatalytic oxidation of NADH. Electrochim Acta 45:3951–3957
49. Piela B, Wrona PK (2002) Oxidation of nitrites on solid electrodes. I. Determination of the reaction mechanism on the pure electrode surface. J Electrochem Soc 149:E55–E63
50. Fox JB (1985) The determination of nitrite. A critical review. Crit Rev Anal Chem 15:283–313